JOC The Journal of Organic Chemistry

Article

pubs.acs.org/joc

Double Role of the Hydroxy Group of Phosphoryl in Palladium(II)-Catalyzed *ortho*-Olefination: A Combined Experimental and Theoretical Investigation

Liu Liu,[†] Hang Yuan,[†] Tingting Fu,[†] Tao Wang,[†] Xiang Gao,[§] Zhiping Zeng,[§] Jun Zhu,*[,‡] and Yufen Zhao*[,†]

[†]Department of Chemistry, College of Chemistry and Chemical Engineering, Key Laboratory for Chemical Biology of Fujian Province, and Collaborative Innovation Center of Chemistry for Energy Materials (iChEM), Xiamen University, Xiamen 361005, Fujian, China

[‡]State Key Laboratory of Physical Chemistry of Solid Surfaces and Fujian Provincial Key Laboratory of Theoretical and Computational Chemistry, College of Chemistry and Chemical Engineering, Xiamen University, Xiamen 361005, Fujian, China

[§]School of Pharmaceutical Sciences, Xiamen University, Xiamen 361102, Fujian, China

Supporting Information

ABSTRACT: Density functional theory calculations have been carried out on Pd-catalyzed phosphoryl-directed *ortho*-olefination to probe the origin of the significant reactivity difference between methyl hydrogen benzylphosphonates and dimethyl benzylphosphonates. The overall catalytic cycle is found to include four basic steps: C−H bond activation, transmetalation, reductive elimination, and recycling of catalyst, each of which is constituted from different steps. Our calculations reveal that the hydroxy group of phosphoryl plays a crucial role almost in all steps, which can not only stabilize the intermediates and transition states by intramolecular hydrogen bonds but also act as a proton donor so that the η^1-CH_3COO^- ligand could be protonated to form a neutral acetic acid for easy removal. These findings explain why only the methyl hydrogen benzylphosphonates and methyl hydrogen phenylphosphates were found to be suitable reaction partners. Our mechanistic findings are further supported by theoretical prediction of Pd-catalyzed *ortho*-olefination using methyl hydrogen phenylphosphonate, which is verified by experimental observations that the desired product was formed in a moderate yield.

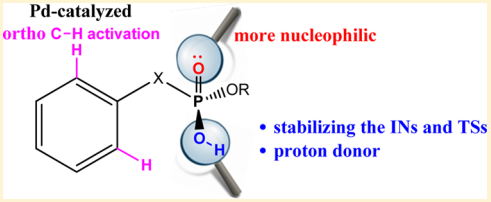

1. INTRODUCTION

The transition-metal-catalyzed cross-coupling reactions, such as Heck,[1] Negishi,[2] and Suzuki−Miyaura[3] reactions, are very useful protocols for the creation of C−C and C−heteroatom bonds. These methods have been extensively studied, and some of them have proven to be exploited in the fine chemical, agrochemical, and pharmaceutical industries.[4] However, two disadvantages for these types of transformations are poor atom economy and nongreen halogen byproducts.[5] Since 2000, transition-metal-catalyzed C−H bond activation reactions have attracted increasing attention owing to the high efficiency and atom economy for C−C bond and C−heteroatom bond formation.[6] Gratifyingly, several distinct C−H functionalization strategies have been successfully applied in natural products synthesis.[7] To gain more insight into these important reaction mechanisms, a number of experimental[8] and theoretical[9] studies were carried out. The common acceptable mechanism involves four basic steps: C−H activation, transmetalation, reductive elimination, and recycling of catalyst (Scheme 1).

Recently, the directing groups such as carboxyl[10] and hydroxyl[11] have been widely utilized for transition-metal-catalyzed *ortho*-C−H activation reactions, providing a potentially useful procedure for the construction of structurally sophisticated compounds. For instance, Kim and co-workers reported a phosphoryl-directed Pd-catalyzed *ortho*-olefination (Scheme 2).[12] It is very interesting to note that methyl hydrogen benzylphosphonate (**1a**) and methyl hydrogen phenylphosphate (**1b**) were found to be suitable reaction partners, whereas dimethyl benzylphosphonate (**2a**) and dimethyl phenylphosphate (**2b**) as the substrates did not give *ortho*-olefination products under the same reaction conditions.[12] Although a plausible reaction mechanism was proposed by the authors,[12b] however, many questions remain elusive, for instance: (i) How does each of the catalytic steps take place?

Scheme 1. Common Acceptable Mechanism of Transition-Metal-Catalyzed C−H Bond Activation Reactions

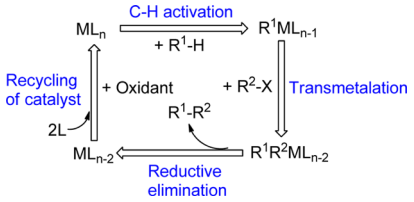

Received: October 15, 2013
Published: December 5, 2013

   dx.doi.org/10.1021/jo402307x | J. Org. Chem. 2014, 79, 80−87

Scheme 2. Phosphoryl-Related Directed Pd-Catalyzed *ortho*-Olefination

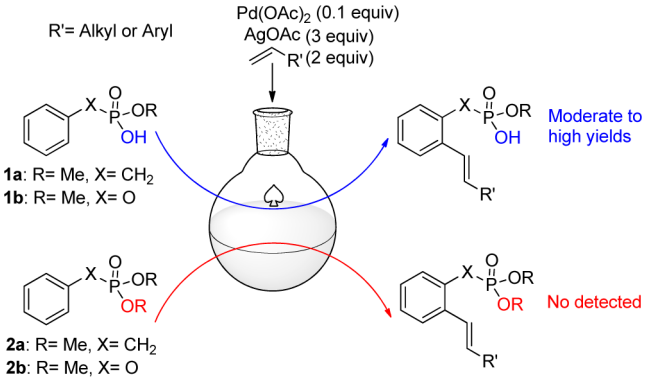

(ii) What is the barrier for each step? (iii) Why are methyl hydrogen benzylphosphonates and methyl hydrogen phenylphosphates more reactive than dimethyl benzylphosphonates and dimethyl phenylphosphates? (iv) Why does AgOAc improve the reaction significantly? Herein, our ongoing interest in organophosphorus chemistry[13] has led us to investigate the detailed reaction mechanisms on the different reactivities of the substrates summarized by Scheme 2.

2. COMPUTATIONAL DETAILS

In the density functional theory (DFT) calculations, geometry optimizations and frequency calculations were performed via the Gaussian 03 programs.[14a] DFT method B3PW91,[15] which has been chosen in recent mechanistic studies on Pd-catalyzed reactions,[16] with a mixed basis set employing 6-31+G(d)[17] for C, H, and O and LANL2DZ[18] for P, Pd, and Ag were used. Polarization functions were added for P (ξ_d = 0.387), Pd (ξ_f = 1.472), and Ag (ξ_f = 1.611) to the standard LANL2DZ basis set.[19] Transition states were examined by vibrational analysis and then submitted to intrinsic reaction coordinate (IRC) calculations to determine two corresponding minima. Energies in solution (1,4-dioxane) have been calculated by means of single-point calculations (IEF-PCM method with the Bondi radii)[20] via the Gaussian 09 program[14b] with the B3PW91 method using the SDD[21] pseudopotential for the metal center and the extended 6-311++G(2d,p)[22] basis set for the other atoms. The gas-phase geometry was used for all of the solution-phase calculations. A similar treatment was also used in many

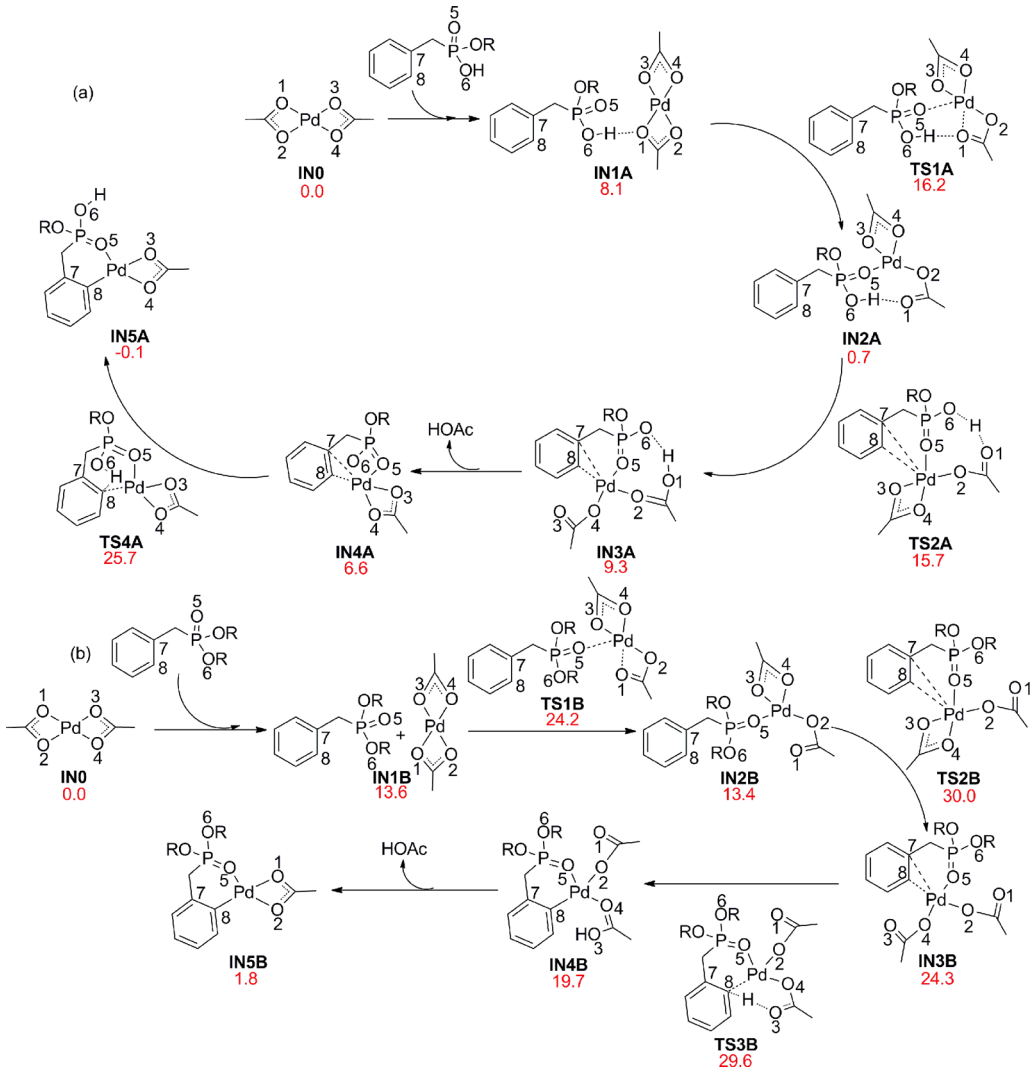

Figure 1. Free energy profile for the C−H activation step for Pd(II)-catalyzed *ortho*-olefination of methyl hydrogen benzylphosphonates (a) and dimethyl benzylphosphonates (b) (R = Me). The energies are given in kcal/mol.

dx.doi.org/10.1021/jo402307x | J. Org. Chem. 2014, 79, 80−87

recent computational studies.[23] The free energy correction from frequency calculation was added to the single-point energy to obtain the free energy in solution. All the solution-phase free energies reported herein correspond to the reference state of 1 mol/L, 298 K.

3. RESULTS AND DISCUSSION

3.1. C−H Bond Activation. The model substrate methyl hydrogen benzylphosphonate (**1a**), dimethyl benzylphosphonate (**2a**), styrene, catalyst $Pd(OAc)_2$, and oxdant AgOAc were chosen. Relative free energies in solution (1,4-dioxane) are employed to analyze the reaction mechanism. Figure 1 depicts the C−H bond activation step for Pd(II)-catalyzed *ortho*-olefination of methyl hydrogen benzylphosphonates (Figure 1a) and dimethyl benzylphosphonates (Figure 1b), respectively. In 2007, Yu and co-workers reported the first carbonyl-directed Pd-catalyzed *ortho*-C−H bond activation/C−C coupling reactions and mechanistic rationalization of unusual kinetics in Pd-catalyzed C−H olefination.[24h,i] On the basis of their findings and previous proposed mechanisms,[24] the reaction may start when **1a** combines with the $Pd(OAc)_2$ catalyst, concomitant with an $\eta^2 \rightarrow \eta^1$ hapticity change in the CH_3COO^- ligand. Three transition states were identified for this transformation (Figure 2), because **1a** has different P-

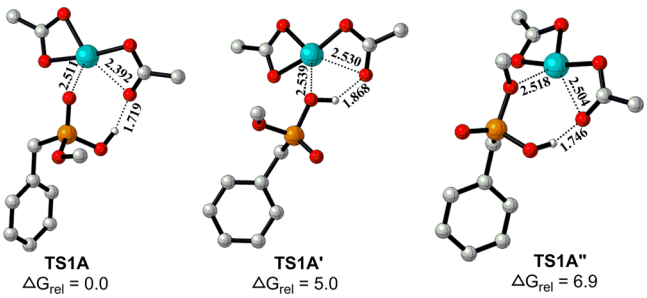

Figure 2. Structures and relative free energies of three transition states with different oxygen atoms binding to the Pd center.[25] For clarity, the hydrogens of C−H are not shown. Bond lengths are given in Å and energies in kcal/mol.

bonded oxygen atoms, which can use their lone pairs to coordinate to the Pd center, respectively. Our calculations show that the most favorable process occurs when the oxygen atom of P═O attacks the Pd center (**TS1A**). The free energy of **TS1A** is lower than those of **TS1A′** and **TS1A′′** by 5.0 and 6.9 kcal/mol, respectively. In addition, natural bond orbital (NBO)[26] analysis shows that negative charges of three oxygens in **1a** are −1.13 (P═O), −1.06 (P−O−H), and −0.88 (P−O−Me), respectively, indicating that the oxygen of P═O is more nucleophilic. Thus, **TS1A** was selected for the further study.

Initially, model substrate methyl hydrogen benzylphosphonate (Figure 1a) binds to the $Pd(OAc)_2$ catalyst to produce a complex **IN1A** by a hydrogen bond O6−H···O1 with a positive energy of 8.1 kcal/mol. Our calculations show that this complexation is a endergonic process and the major contribution to the free energy comes from the entropy changes.[27] From **IN1A**, a pentacoordinated Pd(II) transition state **TS1A** is located with a distorted tetragonal pyramid structure. Then a four-coordinated Pd(II) complex **IN2A** (0.7 kcal/mol) is formed, where the O5 uses its lone pair to coordinate to the Pd center. The overall barrier from **IN0** to **TS1A** is 16.2 kcal/mol. On the basis of the complex-induced proximity effect proposed by Beak and Snieckus[28] and the first C−H insertion intermediate from simple carboxylic acids isolated by Yu,[8h] the substrate C7−C8 bond subsequently coordinates to the Pd center to form **IN3A** via the **TS2A** transition state (activation barrier is 15.0 kcal/mol).

In a similar way, model substrate dimethyl benzylphosphonate (Figure 1b) forms a complex **IN1B** with the $Pd(OAc)_2$. After several steps, a four-coordinated Pd(II) complex **IN3B** with two η^1-CH_3COO^- ligands is generated with a higher free energy of 24.3 kcal/mol than **IN0**. It is important to note that the hydroxy group of phosphoryl can assist the first two steps. When dimethyl benzylphosphonate was chosen as model substrate, the free energy of cooresponding transition states (**TS1B** and **TS2B**) are 8.0 and 14.3 kcal/mol higher than those of **TS1A** and **TS2A**, respectively, which can be mainly attributed to the activation of the Pd−O1 bond and stabilizing the corresponding transition states by an intramolecular hydrogen bond O6−H···O1. For instance, the Pd−O1 bond length (2.064 Å) in **IN1A** is longer than that (2.053 Å) in **IN1B**. Furthermore, the Pd−C8 bond length (2.622 Å) in **TS2B** is much shorter than that (2.741 Å) in **TS2A**, indicating that **IN2B** requires more energy to reach **TS2B**. The corresponding intermediate **IN3A** is more stable than **IN3B** by 15.0 kcal/mol. Interestingly, **IN3A** (9.3 kcal/mol) formed through **TS2A** is feathered by not only an η^2-complex but also a spontaneous hydrogen transfer from O6 to O1, forming an intramolecular hydrogen bond O6···H−O1, which could subsequently generate a more stable intermediate **IN4A** (6.6 kcal/mol relative to **IN0**) via the removal of the neutral acetic acid.

The final step in the C−H activation process of **1a** is accomplished by forming a new intermediate **IN5A** (−0.1 kcal/mol relative to **IN0**) via the **TS4A** structure. In **TS4A**, the bond lengths of Pd−C8, C8−H, and H−O5 are 2.121, 1.345 and 1.368 Å. In contrast to the process of **2a**, intermediate **IN3B** proceeds through a intramolecular six-membered transition state **TS3B**, which involves the cleavage of the C8−H bond and the η^1-CH_3COO^--mediated hydrogen transfer, forming a new intermediate **IN4B** (19.7 kcal/mol relative to **IN0**). After the removal of the neutral acetic acid, a more stable intermediate **IN5B** is generated.

Comparing the possible C−H bond activation pathways of the two substrates **1a** and **2a**, one can realize that the hydroxy group of phosphoryl plays a key role in the first C−H activation step. It not only stabilizes the intermediates and transition states by an intramolecular hydrogen bond but also acts as a proton donor so that the η^1-CH_3COO^- ligand could be protonated to form a neutral acetic acid for easy removal. Thus, the free energies of the intermediates and transition states of **1a** (Figure 1a) are much lower than those of **2a** (Figure 1b). As a consequence, activation of the C−H bond in **1a** is more favorable than that in **2a** both kinetically and thermodynamically.

3.2. Transmetalation and Reductive Elimination. The transmetalation and reductive elimination steps (Figures 3 and 4) start with the dissociation of the η^2-CH_3COO^- ligand to create a vacant coordination site on Pd(II) and allow the coordination of the C−C double bond of styrene. **IN5A** can form two different η^2-coordinated intermediates with styrene depending on the orientation of the phenyl ring relative to the CH_3COOH ligand (Figure 3, **A-IN6A** and **B-IN6A**). Gratifyingly, the hydroxy of phosphoryl also plays a crucial role in the $\eta^2 \rightarrow \eta^1$ hapticity change in the CH_3COO^- ligand and

dx.doi.org/10.1021/jo402307x | J. Org. Chem. 2014, 79, 80−87

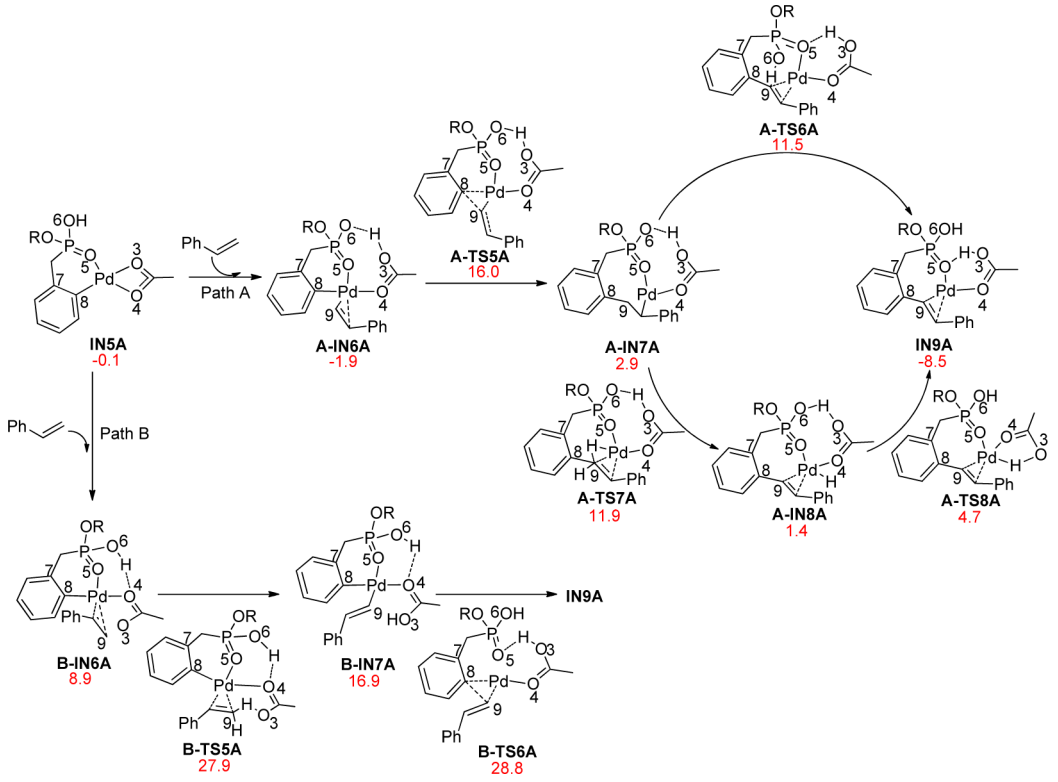

Figure 3. Free energy profile for the transmetalation and reductive elimination steps using methyl hydrogen benzylphosphonate (**1a**) as model substrate. The free energies are given in kcal/mol.

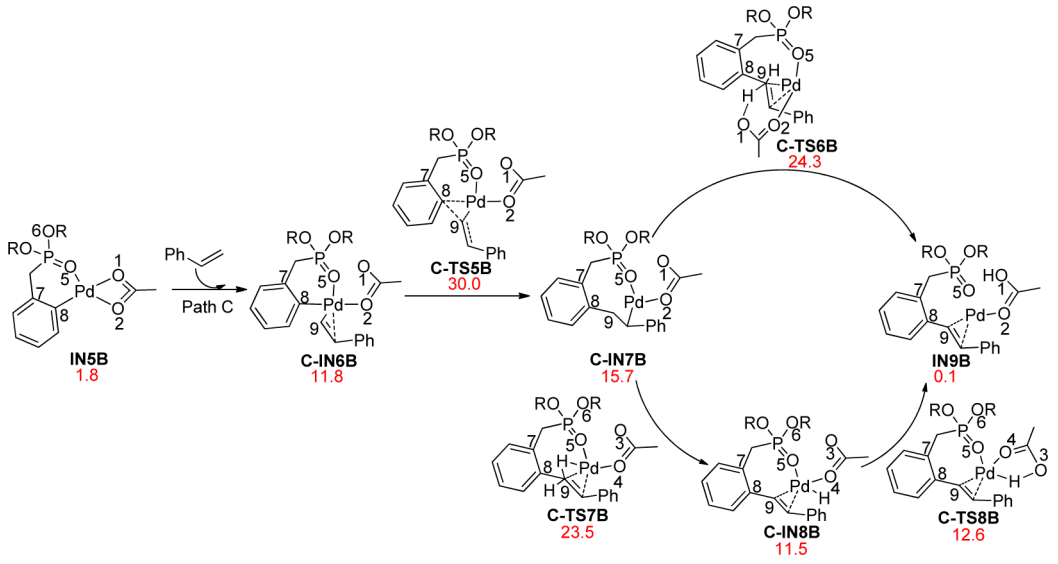

Figure 4. Free energy profile for the transmetalation and reductive elimination steps using dimethyl benzylphosphonate (**2a**) as model substrate. The free energies are given in kcal/mol.

stabilizing intermediates and transition states. For example, from **IN5A**, the η^2-CH_3COO^- ligand dissociation and C−C double bond coordination give η^2-Pd(II) intermediate **A-IN6A** that is exothermic by −1.8 kcal/mol, concomitant with a hydrogen transfer (O6−H → O3−H), forming an intramolecular hydrogen bond O6···H−O3. The energetically favorable intermediate **A-IN6A** proceeds via a three-membered transition state **A-TS5A** (activation barrier is 17.9 kcal/mol), leading to a complex **A-IN7A**. From **A-IN7A**, two possible reaction routes could be located: (i) Direct hydrogen transfer from C9 to O6 through transition state **A-TS6A** with an activation barrier of 8.6 kcal/mol. (ii) Hydrogen transfer from C9 to O3 through two transition states **A-TS7A** (activation barrier of 9.0 kcal/mol for β-H elimination) and **A-TS8A** (activation barrier 3.3 kcal/mol), respectively. Our calculations suggested that these two pathways may occur due to the similar activation barrier, leading to an intermediate **IN9A** (−8.5 kcal/mol relative to **IN0**). Although Path A is energetically accessible under the experimental conditions (383 K),[29] it is necessary to examine Path B (Figure 3) from unfavorable intermediate **B-**

dx.doi.org/10.1021/jo402307x | J. Org. Chem. 2014, 79, 80−87

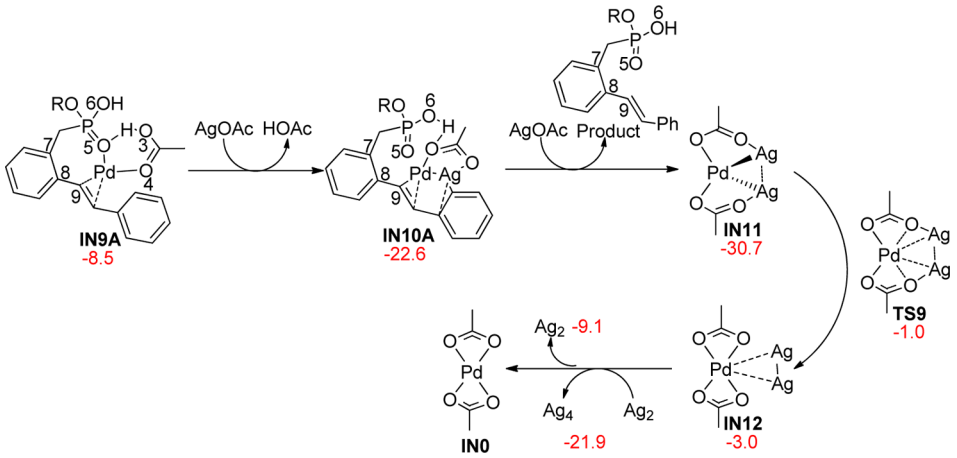

Figure 5. Free energy profile for the recycling of catalyst step (R = Me). The free energies are given in kcal/mol.

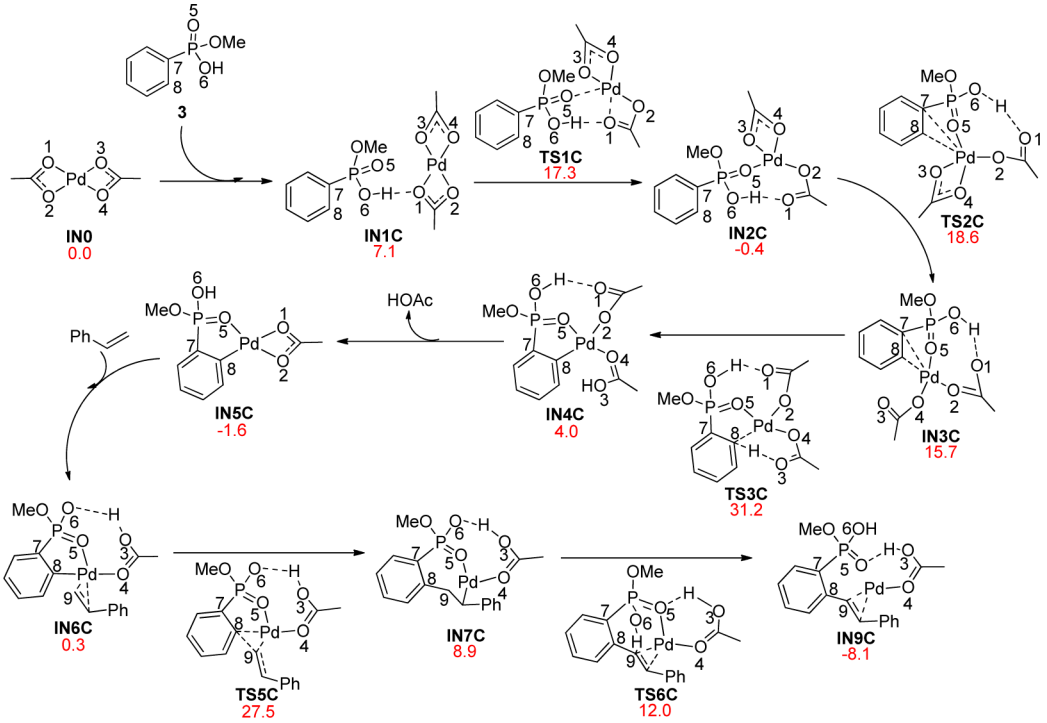

Figure 6. Free energy profile for the Pd-catalyzed *ortho*-olefination using methyl hydrogen phenylphosphonate (**3**). The energies are given in kcal/mol.

IN6A, because a more stable starting material (intermediate) may not lead to a more favorable transition state (Curtin–Hammett Principle).[30] From **B-IN6A**, an η^1-CH_3COO^- transition state **B-TS5A** can be identified with an activation barrier of 19.0 kcal/mol, subsequently forming an unstable intermediate **B-IN7A** (16.9 kcal/mol relative to **IN0**). Next, the reductive elimination takes place by 11.9 kcal/mol, leading to the formation of **IN9A**. Comparing the two possible pathways, we found that the Path B is unfavorable because it is too energy-demanding.

For comparison of two model substrates, a similar pathway of dimethyl benzylphosphonate was also located (Figure 4, path C). The free energy of transtion state **C-TS5B** is computed to be 30.0 kcal/mol, which is 14.0 kcal/mol higher than that of **A-TS5A**. Then the C8–C9 bond formation gives the intermediate **C-IN7B**. Sequentially, the hydrogen was transferred from the C9 atom to the O1 atom via a six-membered transition state **C-TS6B**, leading to the formation of a more stable intermediate **IN9B**. In addition, similar processes may take place from **C-IN7B** through two transition states **C-TS7B** (23.5 kcal/mol) and **C-TS8B** (12.6 kcal/mol), respectively.

In the transmetalation and reductive elimination steps, the activation barrier (17.6 kcal/mol) for the rate-determing step of methyl hydrogen benzylphosphonate is much lower than that (28.2 kcal/mol) of dimethyl benzylphosphonate. Moreover, the process of the **IN5A** → **IN9A** is more exothermic than that of **IN5B** → **IN9B**. The methyl hydrogen benzylphosphonate is again favorable for this transformation, in line with the experimental observations that dimethyl benzylphosphonate was unreactive for the *ortho*-olefination reaction.

3.3. Recycling of Catalyst. Note that, when methyl hydrogen benzylphosphonate was treated with ethyl acrylate (2 equiv) using $Pd(OAc)_2$ (10 mol %) and Ag(I) salts, the reaction was improved significantly.[12] The yields of the *ortho*-

dx.doi.org/10.1021/jo402307x | J. Org. Chem. 2014, 79, 80–87

Scheme 3. Pd-Catalyzed *ortho*-Olefination Using Methyl Hydrogen Phenylphosphonate

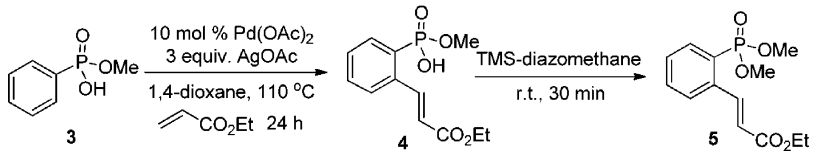

olefination product were changed with the oxidants as follows: AgOAc (2 equiv), 71%; Ag_2CO_3 (2 equiv), 32%; Ag_2O (2 equiv), 57%; and AgOAc (3 equiv), 95%. To investigate the role of AgOAc in the reaction, we turn our attention to the recycling of the $Pd(OAc)_2$ catalyst step. As shown in Figure 5, it starts with a more stable intermediate **IN10A** (−22.6 kcal/mol) via a removal of one CH_3COOH molecule from **IN9A**, followed by a coordination with AgOAc. As experimental study[31] showed that the Ag−Ag bond is relatively strong (bond dissociation energy is 38.3 kcal/mol), the formation of Ag_2 might be facile in the oxidation process. Indeed, when AgOAc was further added, a relatively more stable intermediate **IN11** (−30.7 kcal/mol) was formed. Then the recycling of the catalyst $Pd(OAc)_2$ was achieved by a transition state **TS9**. The barrier from **IN11** to **TS9** is +29.7 kcal/mol, in line with the experimental observation that this *ortho*-olefination reaction was carried out at 110 °C.[29] Finally, separation of Ag_2 leads to regenerate the catalyst $Pd(OAc)_2$ and Ag_2 could build up as the reaction proceeds,[32] facilitating a forward shift in chemical equilibrium.

3.4. Theoretical Prediction and Experimental Realization. Pd-catalyzed C−H bond activation reactions involving a variety of substrates have been studied by various groups, and cyclopalladated compounds were proposed for the transformations.[24] It is worth noting that, in our mechanistic study, all cyclopalladated complexes have a six-membered ring. Interestingly, several stable five-memebered cyclopalladated complexes were prepared in the previous studies.[33,8h] Can the five-membered cyclopalladated complexes be the intermediates or transition states in Pd-catalyzed *ortho*-olefination? To test this hypothesis, we first investigate the reaction mechanism with methyl hydrogen phenylphosphonate (**3**) as the substrate theoretically. As shown in Figure 6, the computed reaction barrier is comparable to that with **1a** as the substrate. Thus, the substrate **3** is predicated to be reactive in Pd-catalyzed *ortho*-olefination.

To verify this predication, we treated methyl hydrogen phenylphosphonate (**3**) (0.2 mmol) and ethyl acrylate (0.4 mmol) with a mixture of $Pd(OAc)_2$ (0.02 mmol) and AgOAc (0.6 mmol), in 1,4-dioxane at 110 °C for 24 h (Scheme 3). ^{31}P NMR and ESI-MS analyses of the crude product showed that the *ortho*-olefination product **4** was obtained, along with the 30% unchanged reactant. For facile purifications, the crude product was methylated by TMS-diazomethane, leading to the methylated product **5** in 66% isolated yield. Not surprisingly, dimethyl phenylphosphonate did not participate in the reaction since no coupled product could be detected in the crude reaction mixture.

4. CONCLUSION

In summary, we have investigated the complete catalytic cycles of palladium(II)-catalyzed phosphoryl-directed *ortho*-olefination by DFT calculations. Our calculation results reveal that the hydroxy group of phosphoryl plays a crucial role almost in all steps, which can not only stabilize the intermediates and transition states by an intramolecular hydrogen bond but also act as a hydrogen donor so that the η^1-CH_3COO^- ligand could be protonated to form a neutral acetic acid for easy removal. These findings explain why only the methyl hydrogen benzylphosphonates and methyl hydrogen phenylphosphates were found to be suitable reaction partners. Our mechanistic studies are further supported by theoretical prediction of Pd-catalyzed *ortho*-olefination using methyl hydrogen phenylphosphonate (**3**), which is verified by experimental observations that the desired product was formed in a moderate yield. These findings provide a useful guide to the design of more efficient directing groups on Pd-catalyzed *ortho*-olefination.

5. EXPERIMENTAL SECTION

5.1. General Information. ^{31}P, ^1H, and ^{13}C NMR spectra were measured on 500 or 400 M spectrometers. ^1H NMR and ^{13}C NMR were recorded using tetramethylsilane (TMS) in the solvent $CDCl_3$ as the internal standard (^1H NMR: TMS at 0.00 ppm, $CHCl_3$ at 7.26 ppm; ^{13}C NMR: $CDCl_3$ at 77.0 ppm) and 85% H_3PO_4 as external standard for ^{31}P NMR. All coupling constants (J values) were reported in hertz (Hz). HRMS spectra were recorded on an FT-MS apparatus.

5.2. Methyl Hydrogen Phenylphosphonate (3). Anhydrous methanol (0.20 mL, 5.0 mmol, 1.0 equiv) was added slowly to an ice-cooled solution of $PhP(O)Cl_2$ (970 mg, 5.0 mmol, 1.0 equiv) in diethyl ether (5.0 mL), followed by the subsequent addition of pyridine (0.40 mL, 5.0 mmol, 1.0 equiv). The white precipitate of pyridine·HCl was filtered off, and the filtrate was concentrated in vacuo. The crude intermediate ($PhP(O)(OMe)Cl$) and 1N NaOH (0.50 mL) were stirred in CH_2Cl_2/H_2O (1:2 v/v, 10 mL) under ambient temperature overnight. The reaction was then extensively extracted with CH_2Cl_2 (10 mL × 5), and the combined organic extract was concentrated in vacuo. The crude residue was purified by flash chromatography (CH_2Cl_2/acetone = 1:2) via a short silica plug to afford the desired product **3**[34] in 90% yield (774 mg). ^1H NMR (500 MHz, $CDCl_3$) δ 7.77−7.87 (m, 2H), 7.51−7.58 (m, 1H), 7.39−7.47 (m, 2H), 3.71 (d, 3H, J = 11.4 Hz); ^{13}C NMR (125 MHz, $CDCl_3$) δ 132.3 (d, J = 3.1 Hz), 131.4 (d, J = 10 Hz), 128.4 (d, J = 15.3 Hz), 128.2 (d, J = 192.7 Hz) and 52.4 (d, J = 5.6 Hz); $^{31}P\{H\}$ NMR (203 MHz, $CDCl_3$) δ 20.9. ESI-MS: $[M + H]^+$ m/z calcd for $C_7H_{10}O_3P^+$: 173.0, found: 173.0.

5.3. (*E*)-Ethyl 3-(2-(dimethoxyphosphoryl)phenyl)acrylate (5). Methyl hydrogen phenylphosphonate **3** (35 mg, 0.2 mmol, 1.0 equiv), $Pd(OAc)_2$ (4.5 mg, 10 mol %), AgOAc (100 mg, 0.6 mmol, 3.0 equiv), ethyl acrylate (40 mg, 0.4 mmol, 2.0 equiv), and dry dioxane (2.0 mL) were mixed in a sealed vial. The reaction mixture was stirred at 110 °C for 24 h. The mixture was then cooled to 0 °C, and 2.0 N HCl solution (1.0 mL) was added. The mixture was extracted with EtOAc (2 × 10 mL). The organic phase was washed with brine, dried over anhydrous $MgSO_4$, and concentrated in vacuo to yield the crude product, which was diluted with methanol (5.0 mL) and treated with TMS-CHN_2 (0.50 mL, 2 M in hexane) at room temperature for 0.5 h. The mixture was evaporated under reduced pressure and purified by silica gel flash column chromatography (hexane/ethyl acetate = 2:1) to afford product **5** in 66% yield (38 mg). ^1H NMR (400 MHz, $CDCl_3$) δ 8.35−8.25 (d, 1H, J = 15.8 Hz), 8.06−7.99 (m, 1H), 7.84−7.77 (m, 1H), 7.60−7.49 (m, 2H), 6.41−6.34 (d, 1H, J = 15.8), 4.32−4.24 (q, 2H, J = 7.2 Hz), 3.77−3.81 (d, 6H, J = 11.2 Hz), 1.36−1.32 (t, 3H, J = 7.2 Hz); ^{13}C NMR (100 MHz, $CDCl_3$) δ 166.4, 142.5 (d, J = 4.7 Hz), 138.0, 134.6 (d, J = 9.4 Hz), 132.9 (d, J = 2.6 Hz), 131.9 (d, J = 9.6 Hz), 129.2 (d, J = 14.7 Hz), 126.7 (d, J = 186.1 Hz), 121.5, 60.6, 52.6

dx.doi.org/10.1021/jo402307x | J. Org. Chem. 2014, 79, 80−87

(d, J = 6.0 Hz), 14.3; $^{31}P\{H\}$ NMR (162 MHz, $CDCl_3$) δ 20.5. HRMS: $[M + H]^+$ m/z calcd for $C_{13}H_{18}O_5P^+$: 285.08864, found: 285.08815.

■ ASSOCIATED CONTENT

Supporting Information

Copies of ^1H and ^{13}C NMR spectra for compounds **3** and **5** and the Cartesian coordinates for all the species. This material is available free of charge via the Internet at http://pubs.acs.org.

■ AUTHOR INFORMATION

Corresponding Authors

*E-mail: jun.zhu@xmu.edu.cn.
*E-mail: yfzhao@xmu.edu.cn.

Notes

The authors declare no competing financial interest.

■ ACKNOWLEDGMENTS

We acknowledge financial support from the National Basic Research Program of China (2012CB821600, 2013CB910700, and 2011CB808504), the Chinese National Natural Science Foundation (21305115, 21103142, 21172184, 21133007, and 81301888), the Program for New Century Excellent Talents in University (NCET-13-0511), the Program for Changjiang Scholars and Innovative Research Team in University, and the Fundamental Research Funds for the Central Universities (2012121021). We are grateful to Prof. Dr. Sunggak Kim and Dr. Xiangjian Meng at Nanyang Technological University for valuable discussions.

■ REFERENCES

(1) Heck, R. F. *Org. React.* **1982**, *27*, 345−390.
(2) Negishi, E. *Acc. Chem. Res.* **1982**, *15*, 340−345.
(3) Miyaura, N.; Yamada, K.; Suzuki, A. *Tetrahedron Lett.* **1979**, *20*, 3437−3440.
(4) Torborg, C.; Beller, M. *Adv. Synth. Catal.* **2009**, *351*, 3027−3043.
(5) Selected recent reviews: (a) Chen, X.; Engle, K. M.; Wang, D.-H.; Yu, J.-Q. *Angew. Chem., Int. Ed.* **2009**, *48*, 5094−5115. (b) Jana, R.; Pathak, T. P.; Sigman, M. S. *Chem. Rev.* **2011**, *111*, 1417−1492. (c) Beletskaya, I. P.; Ananikov, V. P. *Chem. Rev.* **2011**, *111*, 1596−1636. (d) Valente, C.; Çalimsiz, S.; Hoi, K. H.; Mallik, D.; Sayah, M.; Organ, M. G. *Angew. Chem., Int. Ed.* **2012**, *51*, 3314−3332. (e) Han, F.-S. *Chem. Soc. Rev.* **2013**, *42*, 5270−5298. (f) Rosen, B. M.; Quasdorf, K. W.; Wilson, D. A.; Zhang, N.; Resmerita, A.-M.; Garg, N. K.; Percec, V. *Chem. Rev.* **2011**, *111*, 1346−1416.
(6) Selected recent publications: (a) Arockiam, P. B.; Bruneau, C.; Dixneuf, P. H. *Chem. Rev.* **2012**, *112*, 5879−5918. (b) Pandey, G.; Pal, S.; Laha, R. *Angew. Chem., Int. Ed.* **2013**, *52*, 5146−5149. (c) Wang, H.; Schröder, N.; Glorius, F. *Angew. Chem., Int. Ed.* **2013**, *52*, 5386−5389. (d) Chan, L. Y.; Cheong, L.; Kim, S. *Org. Lett.* **2013**, *15*, 2186−2189. (e) Valpuesta, J. E. V.; Álvarez, E.; López-Serrano, J.; Maya, C.; Carmona, E. *Chem.—Eur. J.* **2012**, *18*, 13149−13159. (f) Brasse, M.; Cámpora, J.; Ellman, J. A.; Bergman, R. G. *J. Am. Chem. Soc.* **2013**, *135*, 6427−6430. (g) Cheng, X.-F.; Li, Y.; Su, Y.-M.; Yin, F.; Wang, J.-Y.; Sheng, J.; Vora, H. U.; Wang, X.-S.; Yu, J.-Q. *J. Am. Chem. Soc.* **2013**, *135*, 1236−1239. (h) Cho, K.-B.; Wu, X.; Lee, Y.-M.; Kwon, Y. H.; Shaik, S.; Nam, W. *J. Am. Chem. Soc.* **2012**, *134*, 20222−20225. (i) Maleckis, A.; Kampf, J. W.; Sanford, M. S. *J. Am. Chem. Soc.* **2013**, *135*, 6618−6625. (j) Feng, C.-G.; Ye, M.; Xiao, K.-J.; Li, S.; Yu, J.-Q. *J. Am. Chem. Soc.* **2013**, *135*, 9322−9325. (k) Wang, X.-C.; Hu, Y.; Bonacorsi, S.; Hong, Y.; Burrell, R.; Yu, J.-Q. *J. Am. Chem. Soc.* **2013**, *135*, 10326−10329. (l) Chary, B. C.; Kim, S.; Park, Y.; Kim, J.; Lee, P. H. *Org. Lett.* **2013**, *15*, 2692−2695. (m) Zhao, D.; Nimphius, C.; Lindale, M.; Glorius, F. *Org. Lett.* **2013**, *15*, 4504−4507. (n) Seo, J.; Park, Y.; Jeon, I.; Ryu, T.; Park, S.; Lee, P. H. *Org. Lett.* **2013**, *15*, 3358−3361. (o) Park, S.; Seo, B.; Shin, S.; Son, J.-Y.; Lee, P. H. *Chem. Commun.* **2013**, *49*, 8671−8673.
(7) Selected recent publications: (a) Stang, E. M.; White, M. C. *Nat. Chem.* **2009**, *1*, 547−551. (b) Chen, K.; Baran, P. S. *Nature* **2009**, *459*, 824−828. (c) Rosen, B. R.; Simke, L. R.; Thuy-Boun, P. S.; Dixon, D. D.; Yu, J.-Q.; Baran, P. S. *Angew. Chem., Int. Ed.* **2013**, *52*, 7317−7320. (d) Mandal, D.; Yamaguchi, A. D.; Yamaguchi, J.; Itami, K. *J. Am. Chem. Soc.* **2011**, *133*, 19660−19663.
(8) (a) Jensen, M. P.; Wick, D. D.; Reinartz, S.; White, P. S.; Templeton, J. L.; Goldberg, K. I. *J. Am. Chem. Soc.* **2003**, *125*, 8614−8624. (b) Lafrance, M.; Rowley, C. N.; Woo, T. K.; Fagnou, K. *J. Am. Chem. Soc.* **2006**, *128*, 8754−8756. (c) García-Cuadrado, D.; de Mendoza, P.; Braga, A. A. C.; Maseras, F.; Echavarren, A. M. *J. Am. Chem. Soc.* **2007**, *129*, 6880−6886. (d) Li, L.; Brennessel, W. W.; Jones, W. D. *Organometallics* **2009**, *28*, 3492−3500. (e) Walstrom, A.; Pink, M.; Tsvetkov, N. P.; Fan, H.; Ingleson, M.; Caulton, K. G. *J. Am. Chem. Soc.* **2005**, *127*, 16780−16781. (f) Asplund, M. C.; Snee, P. T.; Yeston, J. S.; Wilkens, M. J.; Payne, C. K.; Yang, H.; Kotz, K. T.; Frei, H.; Bergman, R. G.; Harris, C. B. *J. Am. Chem. Soc.* **2002**, *124*, 10605−10612. (g) Engle, K. M.; Wang, D.-H.; Yu, J.-Q. *J. Am. Chem. Soc.* **2010**, *132*, 14137−14151. (h) Chai, D. I.; Thansandote, P.; Lautens, M. *Chem.—Eur. J.* **2011**, *17*, 8175−8188. (i) Giri, R.; Yu, J.-Q. *J. Am. Chem. Soc.* **2008**, *130*, 14082−14083. (j) Lyons, T. W.; Sanford, M. S. *Chem. Rev.* **2010**, *110*, 1147−1169.
(9) (a) Boutadla, Y.; Davies, D. L.; Macgregor, S. A.; Poblador-Bahamonde, A. I. *Dalton Trans.* **2009**, 5820−5831. (b) Reinhold, M.; McGrady, J. E.; Perutz, R. N. *J. Am. Chem. Soc.* **2004**, *126*, 5268−5276. (c) Zhang, L.; Fang, D.-C. *J. Org. Chem.* **2013**, *78*, 2405−2412. (d) Yang, X.; Hall, M. B. *J. Phys. Chem. A* **2009**, *113*, 2152−2157. (e) Clot, E.; Eisenstein, O.; Jasim, N.; Macgregor, S. A.; McGrady, J. E.; Perutz, R. N. *Acc. Chem. Res.* **2011**, *44*, 333−348. (f) Davies, D. L.; Donald, S. M. A.; Macgregor, S. A. *J. Am. Chem. Soc.* **2005**, *127*, 13754−13755. (g) Pascual, S.; de Mendoza, P.; Braga, A. A. C.; Maseras, F.; Echavarren, A. M. *Tetrahedron* **2008**, *64*, 6021−6029. (h) Balcells, D.; Clot, E.; Eisenstein, O. *Chem. Rev.* **2010**, *110*, 749−823. (i) Lian, B.; Zhang, L.; Chass, G. A.; Fang, D.-C. *J. Org. Chem.* **2013**, *78*, 8376−8385. (j) Giri, R.; Lan, Y.; Liu, P.; Houk, K. N.; Yu, J.-Q. *J. Am. Chem. Soc.* **2012**, *134*, 14118−14126.
(10) Selected recent publications: (a) Ackermann, L.; Pospech, J. *Org. Lett.* **2011**, *13*, 4153−4155. (b) Wang, D.-H.; Engle, K. M.; Shi, B.-F.; Yu, J.-Q. *Science* **2010**, *327*, 315−319. (c) Engle, K. M.; Wang, D.-H.; Yu, J.-Q. *Angew. Chem., Int. Ed.* **2010**, *49*, 6169−6173. (d) Shi, B.-F.; Zhang, Y.-H.; Lam, J. K.; Wang, D.-H.; Yu, J.-Q. *J. Am. Chem. Soc.* **2009**, *132*, 460−461. (e) Xiao, B.; Fu, Y.; Xu, J.; Gong, T.-J.; Dai, J.-J.; Yi, J.; Liu, L. *J. Am. Chem. Soc.* **2009**, *132*, 468−469. (f) Satoh, T.; Miura, M. *Synthesis* **2010**, 3395−3409. (g) Zhang, Y.-H.; Shi, B.-F.; Yu, J.-Q. *Angew. Chem., Int. Ed.* **2009**, *48*, 6097−6100. (h) Wang, D.-H.; Mei, T.-S.; Yu, J.-Q. *J. Am. Chem. Soc.* **2008**, *130*, 17676−17677. (i) Mei, T.-S.; Giri, R.; Maugel, N.; Yu, J.-Q. *Angew. Chem., Int. Ed.* **2008**, *47*, 5215−5219. (j) Ueura, K.; Satoh, T.; Miura, M. *Org. Lett.* **2007**, *9*, 1407−1409. (k) Boele, M. D. K.; van Strijdonck, G. P. F.; de Vries, A. H. M.; Kamer, P. C. J.; de Vries, J. G.; van Leeuwen, P. W. N. M. *J. Am. Chem. Soc.* **2002**, *124*, 1586−1587. (l) Miura, M.; Tsuda, T.; Satoh, T.; Pivsa-Art, S.; Nomura, M. *J. Org. Chem.* **1998**, *63*, 5211−5215. (m) Mochida, S.; Hirano, K.; Satoh, T.; Miura, M. *Org. Lett.* **2010**, *12*, 5776−5779. (n) Li, Y.; Ding, Y.-J.; Wang, J.-Y.; Su, Y.-M.; Wang, X.-S. *Org. Lett.* **2013**, *15*, 2574−2577.
(11) Selected recent publications: (a) Lu, Y.; Leow, D.; Wang, X.; Engle, K. M.; Yu, J.-Q. *Chem. Sci.* **2011**, *2*, 967−971. (b) Wang, X.; Lu, Y.; Dai, H.-X.; Yu, J.-Q. *J. Am. Chem. Soc.* **2010**, *132*, 12203−12205. (c) Lu, Y.; Wang, D.-H.; Engle, K. M.; Yu, J.-Q. *J. Am. Chem. Soc.* **2010**, *132*, 5916−5921.
(12) (a) Chan, L. Y.; Kim, S.; Ryu, T.; Lee, P. H. *Chem. Commun.* **2013**, *49*, 4682−4684. (b) Meng, X.; Kim, S. *Org. Lett.* **2013**, *15*, 1910−1913. (c) Chan, L. Y.; Meng, X.; Kim, S. *J. Org. Chem.* **2013**, *78*, 8826−8832.
(13) Selected recent publications: (a) Gao, Y.; Wang, G.; Chen, L.; Xu, P.; Zhao, Y.; Zhou, Y.; Han, L.-B. *J. Am. Chem. Soc.* **2009**, *131*, 7956−7957. (b) Gao, Y.; Huang, Z.; Zhuang, R.; Xu, J.; Zhang, P.;

Tang, G.; Zhao, Y. *Org. Lett.* **2013**, *15*, 4214−4217. (c) Chen, H.; Huang, Z.; Hu, X.; Tang, G.; Xu, P.; Zhao, Y.; Cheng, C.-H. *J. Org. Chem.* **2011**, *76*, 2338−2344. (d) Gao, X.; Wu, H.; Lee, K.-C.; Liu, H.; Zhao, Y.; Cai, Z.; Jiang, Y. *Anal. Chem.* **2012**, *84*, 10236−10244. (e) Liu, L.; Wang, Y.; Zeng, Z.; Xu, P.; Gao, Y.; Yin, Y.; Zhao, Y. *Adv. Synth. Catal.* **2013**, *355*, 659−666. (f) Miao, W.; Gao, Y.; Li, X.; Gao, Y.; Tang, G.; Zhao, Y. *Adv. Synth. Catal.* **2012**, *354*, 2659−2664. (g) Zhuang, R.; Xu, J.; Cai, Z.; Tang, G.; Fang, M.; Zhao, Y. *Org. Lett.* **2011**, *13*, 2110−2113. (h) Zhao, Z.; Xue, W.; Gao, Y.; Tang, G.; Zhao, Y. *Chem.—Asian J.* **2013**, *8*, 713−716. (i) Xu, J.; Zhang, P.; Gao, Y.; Chen, Y.; Tang, G.; Zhao, Y. *J. Org. Chem.* **2013**, *78*, 8176−8183. (j) Fu, C.; Zheng, X.; Jiang, Y.; Liu, Y.; Xu, P.; Zeng, Z.; Liu, R.; Zhao, Y. *Chem. Commun.* **2013**, *49*, 2795−2797.

(14) (a) Frisch, M. J.; et al. *Gaussian 03*, Revision E.01; Gaussian, Inc.: Wallingford, CT, 2004. (b) Frisch, M. J.; et al. *Gaussian 09*, Revision B.01; Gaussian, Inc.: Wallingford, CT, 2010.

(15) (a) Becke, A. D. *Phys. Rev. A* **1988**, *38*, 3098. (b) Perdew, J. P.; Burke, K.; Wang, Y. *Phys. Rev. B* **1996**, *54*, 16533.

(16) (a) Dickstein, J. S.; Curto, J. M.; Gutierrez, O.; Mulrooney, C. A.; Kozlowski, M. C. *J. Org. Chem.* **2013**, *78*, 4744−4761. (b) Derrah, E. J.; Martin, C.; Mallet-Ladeira, S.; Miqueu, K.; Bouhadir, G.; Bourissou, D. *Organometallics* **2013**, *32*, 1121−1128. (c) Ho, F.; Li, Y.; Mathey, F. *Organometallics* **2012**, *31*, 8456−8458. (d) Ortiz, D.; Blug, M.; Le Goff, X.-F.; Le Floch, P.; Mézailles, N.; Maître, P. *Organometallics* **2012**, *31*, 5975−5978. (e) Rünzi, T.; Tritschler, U.; Roesle, P.; Göttker-Schnetmann, I.; Möller, H. M.; Caporaso, L.; Poater, A.; Cavallo, L.; Mecking, S. *Organometallics* **2012**, *31*, 8388−8406. (f) Nebra, N.; Saffon, N.; Maron, L.; Martin−Vaca, B.; Bourissou, D. *Inorg. Chem.* **2011**, *50*, 6378−6383. (g) Considering that the B3PW91 functional is problematic in treating some transition-metal systems, we also evaluated the effects of density functionals in this study. The results show that different DFT methods give a consistent picture on the observed selectivity. The data are listed in the Supporting Information.

(17) (a) Ditchfield, R.; Hehre, W. J.; Pople, J. A. *J. Chem. Phys.* **1971**, *54*, 724−728. (b) Hehre, W. J.; Ditchfield, R.; Pople, J. A. *J. Chem. Phys.* **1972**, *56*, 2257−2261. (c) Hariharan, P. C.; Pople, J. A. *Theor. Chim. Acta* **1973**, *28*, 213−222. (d) Dill, J. D.; Pople, J. A. *J. Chem. Phys.* **1975**, *62*, 2921−2923. (e) Francl, M. M.; Pietro, W. J.; Hehre, W. J.; Binkley, J. S.; Gordon, M. S.; DeFrees, D. J.; Pople, J. A. *J. Chem. Phys.* **1982**, *77*, 3654−3665.

(18) Wadt, W. R.; Hay, P. J. *J. Chem. Phys.* **1985**, *82*, 284−298.

(19) (a) Hollwarth, A.; Bohme, M.; Dapprich, S.; Ehlers, A. W.; Gobbi, A.; Jonas, V.; Kohler, K. F.; Stegmann, R.; Veldkamp, A.; Frenking, G. *Chem. Phys. Lett.* **1993**, *208*, 237−240. (b) Ehlers, A.; Böhme, M.; Dapprich, S.; Gobbi, A.; Höllwarth, A.; Jonas, V.; Köhler, K.; Stegmann, R.; Veldkamp, A.; Frenking, G. *Chem. Phys. Lett.* **1993**, *208*, 111−114.

(20) Bondi, A. *J. Phys. Chem.* **1964**, *68*, 441−451.

(21) Fuentealba, P.; Preuss, H.; Stoll, H.; Szentpaly, L. v. *Chem. Phys. Lett.* **1982**, *89*, 418−422.

(22) (a) Krishan, R.; Binkley, J. S.; Seeger, R.; Pople, J. A. *J. Chem. Phys.* **1980**, *72*, 650−654. (b) McLean, A. D.; Chandler, G. S. *J. Chem. Phys.* **1980**, *72*, 5639−5648. (c) Clark, T.; Chandrasekhar, J.; Spitznagel, G. W.; Schleyer, P. V. R. *J. Comput. Chem.* **1983**, *4*, 294−301.

(23) Selected recent publications: (a) Sengupta, A.; Sunoj, R. B. *J. Org. Chem.* **2012**, *77*, 10525−10536. (b) Cho, D.; Ko, K. C.; Lee, J. Y. *Organometallics* **2013**, *32*, 4571−4576. (c) Wang, J.; Liu, B.; Zhao, H.; Wang, J. *Organometallics* **2012**, *31*, 8598−8607. (d) Dang, Y.; Wang, Z.-X.; Wang, X. *Organometallics* **2012**, *31*, 8654−8657. (e) Liu, L.; Zhang, S.; Chen, H.; Lv, Y.; Zhu, J.; Zhao, Y. *Chem.—Asian J.* **2013**, *8*, 2592−2595. (f) Quasdorf, K. W.; Antoft-Finch, A.; Liu, P.; Silberstein, A. L.; Komaromi, A.; Blackburn, T.; Ramgren, S. D.; Houk, K. N.; Snieckus, V.; Garg, N. K. *J. Am. Chem. Soc.* **2011**, *133*, 6352−6363. (g) Blay, G.; Cano, J.; Cardona, L.; Fernández, I.; Muñoz, M. C.; Pedro, J. R.; Vila, C. *J. Org. Chem.* **2012**, *77*, 10545−10556. (h) Ananikov, V. P.; Beletskaya, I. P. *Chem.—Asian J.* **2011**, *6*, 1423−1430.

(24) (a) Wan, J.-C.; Huang, J.-M.; Jhan, Y.-H.; Hsieh, J.-C. *Org. Lett.* **2013**, *15*, 2742−2745. (b) Miao, J.; Ge, H. *Org. Lett.* **2013**, *15*, 2930−2933. (c) Wesch, T.; Berthelot-Bréhier, A.; Leroux, F. R.; Colobert, F. *Org. Lett.* **2013**, *15*, 2490−2493. (d) Dai, H.-X.; Li, G.; Zhang, X.-G.; Stepan, A. F.; Yu, J.-Q. *J. Am. Chem. Soc.* **2013**, *135*, 7567−7571. (e) Li, Y.; Ding, Y.-J.; Wang, J.-Y.; Su, Y.-M.; Wang, X.-S. *Org. Lett.* **2013**, *15*, 2574−2577. (f) Zhang, W.; Lou, S.; Liu, Y.; Xu, Z. *J. Org. Chem.* **2013**, *78*, 5932−5948. (g) Engle, K. M.; Yu, J.-Q. *J. Org. Chem.* **2013**, *78*, 8927−8955. (h) Giri, R.; Maugel, N.; Li, J.-J.; Wang, D.-H.; Breazzano, S. P.; Saunders, L. B.; Yu, J.-Q. *J. Am. Chem. Soc.* **2007**, *129*, 3510−3511. (i) Baxter, R. D.; Sale, D.; Engle, K. M.; Yu, J.-Q.; Blackmond, D. G. *J. Am. Chem. Soc.* **2012**, *134*, 4600−4606.

(25) Legault, C. Y. *CYLview*, 1.0b; Université de Sherbrooke: Sherbrooke, Québec, Canada, 2009; www.cylview.org.

(26) Glendening, E. D.; Reed, A. E.; Carpenter, J. E.; Weinhold, F. *NBO*, Version 3.1.

(27) During the transformations of $Pd(OAc)_2$ + $PhCH_2P(O)(OMe)(OH)$ → **IN1A** (ΔG = 8.1 kcal/mol, ΔH = −2.5 kcal/mol, and ΔS = −148.8 J/mol K) and $Pd(OAc)_2$ + $PhCH_2P(O)(OMe)_2$ → **IN1B** (ΔG = 10.4 kcal/mol, ΔH = 2.3 kcal/mol, and ΔS = −113.7 J/mol K), the major contribution to the free energy comes from the entropy.

(28) Whisler, M. C.; MacNeil, S.; Snieckus, V.; Beak, P. *Angew. Chem., Int. Ed.* **2004**, *43*, 2206−2225.

(29) According to the Eyring equation, i.e., $k = (k_BT/h)\exp(-\Delta G^{‡}/RT)$, where k is the rate constant, k_B is Boltzmann's constant, T is the temperature, $\Delta G^{‡}$ is the activation free energy, R is the gas constant, and h is Planck's constant, we evaluate the barrier. Assuming that the half-life of this reaction is 24 h and the concentration of each reactant is 1 mol/L, we obtain the second-order rate constant k is 1.2×10^{-5} L/mol·s. Therefore, $\Delta G^{‡}$ is 31.4 kcal/mol at 110 °C.

(30) Seeman, J. I. *Chem. Rev.* **1983**, *83*, 83−134.

(31) Huber, K. P.; Herzberg, G. *Molecular Spectra and Molecular Structure I*; Van Nostrand Reinhold: New York, 1950.

(32) (a) The free energy change of $2Ag_2 \rightarrow Ag_4$ is −12.8 kcal/mol. (b) The formation of Ag metal can be detected when the reaction finished.

(33) (a) Cámpora, J.; Palma, P.; del Río, D.; Carmona, E.; Graiff, C.; Tiripicchio, A. *Organometallics* **2003**, *22*, 3345−3347. (b) Cámpora, J.; Palma, P.; del Río, D.; López, J. A.; Álvarez, E.; Connelly, N. G. *Organometallics* **2005**, *24*, 3624−3628. (c) Cámpora, J.; López, J. A.; Palma, P.; del Rio, D.; Carmona, E.; Valerga, P.; Graiff, C.; Tiripicchio, A. *Inorg. Chem.* **2001**, *40*, 4116−4126. (d) Deng, J.; Gao, H.; Zhu, F.; Wu, Q. *Organometallics* **2013**, *32*, 4507−4505. (e) Grande, L.; Serrano, E.; Cuesta, L.; Urriolabeitia, E. P. *Organometallics* **2011**, *31*, 394−404. (f) Racowski, J. M.; Gary, J. B.; Sanford, M. S. *Angew. Chem., Int. Ed.* **2012**, *51*, 3414−3417.

(34) Oh, Y.-C.; Bao, Y.; Jenks, W. S. *J. Photochem. Photobiol., A: Chem.* **2003**, *161*, 69−77.